Photometry of the Martian Surface using data from the Navigation Cameras on the Mars Exploration Rovers *Spirit* and *Opportunity*. J. M. Soderblom[1], J. F. Bell III[1], J. R. Johnson[2], J. N. Maki[3], M. J. Wolff[4], and the Athena Science Team, [1]Cornell University, Space Science Building, Ithaca, NY 14853, jasons@astro.cornell.edu, [2]U.S. Geological Survey, Flagstaff, AZ, [3]Jet Propulsion Laboratory, Pasadena, CA, [4]Space Science Institute, Boulder, CO.

Introduction: The navigation cameras (Navcams) [1] on the Mars Exploration Rovers *Spirit* and *Opportunity* are used nearly every sol in the general operations of the rovers to document the overall geomorphology and topography of the sites, to map the location of the rovers, and to provide data needed for rover driving decisions. In this study we make use of this expansive data set to model the broadband photometric properties of the surface materials at the landing sites using a radiative transfer model based on that described by Hapke [2,3]. Physical properties such as the presence and thickness of rock coatings and air-fall dust porosity derived from these models can then be used to provide constraints on the geologic, aeolian, and climatic history of the region. This project will also provide further constraints on surface physical and photometric properties required for radiative transfer modeling of the atmosphere. Comparison of the results from this project with photometric studies conducted with other lander, rover, and orbiter data sets will help to validate and refine orbital photometry, improving both the quality of these data and the predictive accuracy of orbital photometric studies in assessing potential landing sites as well as global-scale surface physical-properties characteristics.

Observations: The success of the MER missions marks a new opportunity for Mars surface photometry studies. With unprecedented mobility, the two spacecraft have been able to image more of the surface of Mars at sub-cm resolution than any other mission to date. While each rover carries 9 cameras, the Navcam pair has been used more systematically than any of the other cameras to document the geomorphologic properties of each landing site. The Navcams are a stereo pair with a 20 cm baseline mounted atop the rover's mast, about 1.5 m above the surface. Each camera has a 45° field of view with an angular resolution of 0.82 mrad/pixel. Each Navcam has an effective bandpass of ~650 nm (+100, -70 nm) [1].

The Navcams are used to document the landing sites, map the rovers' locations, and provide the rover planners the data needed for driving the rovers . Each time a new "site" is defined during the mission, a new set of Navcam images, frequently a 360° panorama, is obtained. These site surveys are often augmented by additional Navcam images targeted towards specific regions of interest as a prelude to more in-depth Pancam, Mini-TES, or rover arm instrument activities. With 122 different sites sampled in Spirit data and 64 sites sampled in Opportunity data as of this writing, the Navcam images provide the greatest range of illumination and viewing geometries of any of the rover camera datasets (See Figure 1).

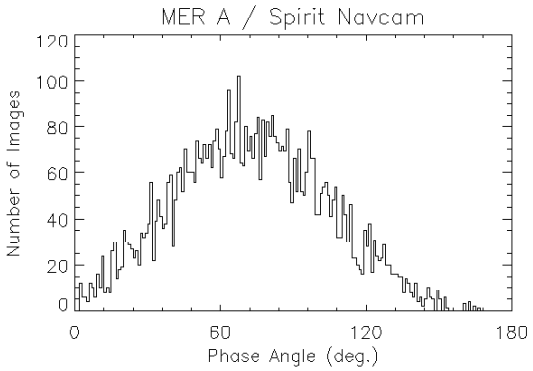

Figure 1. Histogram of the distribution of phase angle coverage for the centers of the fields-of-view of all Navcam images for *Spirit* as of January 2006. This histogram is comprised of over 4000 image pairs.

In addition to these systematic data a dedicated photometric study was conducted on *Spirit* using the Navcams on Sols 660-663 (See Figure 2). Data were acquired at 11 different times of day in the north, south, sunset and anti-sunset directions providing phase coverage from ~1°, (limited by the camera shadow), to ~165° and sampling nearly all incidence angles at an emission angle of 72.5°. Images of the Pancam calibration target [4] were acquired with the Navcams near-in-time to these 11 observations allowing a more accurate radiometric calibration of these data.

Calibration: The MER Navcam images being released by the PDS have had an approximate radiometric calibration applied, using only a scaling factor relative to Pancam images and in some cases a generic flatfield correction. The calibrated images as released have not been corrected for bias, dark current, electronic shutter smear, temperature-dependent responsivity variations, variations in the diffuse illumination component of the radiance, or variations in dust deposition on the calibration target. Based on the approximated nature of the current absolute calibration and comparisons between the

Pancam and Navcam images of the sky and/or the same surface regions, we estimate that the uncertainties on the absolute radiometry of the Navcam images are probably within a factor of 2, but a rigorous assessment of the accuracy and precision of the absolute calibration has not been performed.

A necessary first step in this study is the development of a Navcam calibration pipeline. Based on the Pancam calibration pipeline [4,5] this calibration pipeline will include corrections for instrumental dark current, bias, shutter smear, and flatfield variations, as well as a conversion to units of absolute radiance ($W/m^2/nm/sr$). Numerous Navcam observations that include the Pancam calibration target will also be used to calibrate the images to relative reflectance or R* [6], using the same methods and algorithms that were successfully used for Pancam [4,5]. For rock and soil surfaces parallel to the surface of the Pancam calibration target, R* images calibrated using calibration target images acquired close in time also include a self-correction for the time-variable diffuse illumination component arising from sky radiance.

In addition to the radiometric calibration of Navcam data, we will also run the images through the PANMAP Pancam geometric mapping pipeline [4] so that range, incidence (i), emission (e), and phase angle (g) information can be derived for every pixel in the scene. The mapping pipeline relies on a combination of image pointing information provided in the PDS file labels, a geometric camera model for each instrument [1], and automated stereo correlation of stereo pair images [7].

Modeling: Scattering properties of classes of materials will be modeled using the radiative transfer modeling approach described by Hapke [2,3]. Surface materials will be classified by morphology and albedo into groups such as bright and dark soils, dark angular rocks, bright laminated rocks, and brighter rounded rocks. Using this model we hope to constrain the amplitude and angular widths of the coherent backscatter opposition effect (CBOE) and the shadow-hiding opposition effect (SHOE), the single-scattering albedo, the single-particle phase function, and the macroscopic surface roughness. We will use a two-parameter double Henyey-Greenstein function to describe the single-particle scattering and correct for diffuse, reddened skylight using a DISORT-based model [8].

References: [1] Maki, J.N. et al. (2003) *JGR, 108*, doi:10.1029/2003JE002077. [2] Hapke, B. (1981) *JGR, 86*, 3039-3054. [3] Hapke, B. (2002) *Icarus, 157*, 523-534. [4] Bell, J.F. III et al. (2003) *JGR, 108*, doi:10.1029/2003JE002070. [5] Bell, J.F. III et al. (2006) *JGR, 111*, doi:10.1029/2005JE002444. [6] Reid, R.J. et al. (1999) *JGR, 104*, 8907-8926. [7] Johnson, J.R. et al. (2006) *JGR*, in press. [8] Stamnes K. et al. (1988) *Ap. Opt.*, 27, 2502-2509.

Figure 2. Example images from a Navcam photometry campaign on *Spirit* Sols 630 – 633. Datasets consisting of four image pairs in the north, south, sunset, and anti-sunset directions were acquired at 11 different times of day ranging in phase from 5° (above left) to 149° (above right) at the center of the field of view. In the low-phase image the opposition effect can be observed near the shadow of the Pancam Mast Assembly. In the high-phase image forward scattering is seen. The highly forward scattering nature of the soil compacted by the rover is also evident.